

Example of Highly Stereoregulated Ruthenium Amidine Complex Formation: Synthesis, Crystal Structures, and Spectral and Redox Properties of the Complexes

$[\text{Ru}^{\text{II}}(\text{trpy})\{\text{NC}_5\text{H}_4\text{—CH=N—N}(\text{C}_6\text{H}_5)\text{C}(\text{CH}_3)=\text{NH}\}](\text{ClO}_4)_2$ (**1**) and $[\text{Ru}^{\text{II}}(\text{trpy})(\text{NC}_5\text{H}_4\text{—CH=N—NH—C}_6\text{H}_5)\text{Cl}]\text{ClO}_4$ (**2**) (trpy = 2,2':6',2''-Terpyridine)

Biplab Mondal,[†] Vedavati G. Puranik,[‡] and Goutam Kumar Lahiri^{*†}

Department of Chemistry, Indian Institute of Technology, Bombay, Powai, Mumbai-400076, India, and Physical Chemistry Division, National Chemical Laboratory, Pune, Maharashtra-411008, India

Received May 16, 2002

The reaction of $\text{Ru}(\text{trpy})\text{Cl}_3$ (trpy = 2,2':6',2''-terpyridine) with the pyridine-based imine function $\text{N}_p\text{C}_5\text{H}_4\text{—CH=N—N}_i\text{—NH—C}_6\text{H}_5$ (L), incorporating an NH spacer between the imine nitrogen (N_i) and the pendant phenyl ring, in ethanol medium followed by chromatographic work up on a neutral alumina column using $\text{CH}_3\text{CN}/\text{CH}_2\text{Cl}_2$ (1:4) as eluent, results in complexes of the types $[\text{Ru}(\text{trpy})(\text{L}')](\text{ClO}_4)_2$ (**1**) and $[\text{Ru}(\text{trpy})(\text{L})\text{Cl}]\text{ClO}_4$ (**2**). Although the identity of the free ligand (L) has been retained in complex **2**, the preformed imine-based potentially bidentate ligand (L) has been selectively transformed into a new class of unusual imine–amidine-based tridentate ligand, $\text{N}_p\text{C}_5\text{H}_4\text{—CH=N—N}_i\text{—N}(\text{C}_6\text{H}_5)\text{C}(\text{CH}_3)=\text{N}_a\text{H}$ (L'), in **1**. The single-crystal X-ray structures of the free ligand (L) and both complexes **1** and **2** have been determined. In **2**, the sixth coordination site, that is, the Cl^- function, is cis to the pyridine nitrogen (N_p) of L which in turn places the NH spacer away from the Ru—Cl bond, whereas, in **1**, the corresponding sixth position, that is, the Ru—N_a (amidine) bond, is trans to the pyridine nitrogen (N_p) of L' . The trans configuration of N_a with respect to the N_p of L' in **1** provides the basis for the selective $\text{L} \rightarrow \text{L}'$ transformation in **1**. The complexes exhibit strong $\text{Ru}(\text{II}) \rightarrow \pi^*$ (trpy) MLCT transitions in the visible region and intraligand transitions in the UV region. The lowest energy MLCT band at 510 nm for **2** has been substantially blue-shifted to 478 nm in the case of **1**. The reversible $\text{Ru}(\text{III})\text{—Ru}(\text{II})$ couples for **1** and **2** have been observed at 0.80 and 0.59 V versus SCE, respectively. The complexes are weakly luminescent at 77 K, exhibiting emissions at λ_{max} , 598 nm [quantum yield (Φ) = 0.43×10^{-2}] and 574 nm ($\Phi = 0.28 \times 10^{-2}$) for **1** and **2**, respectively.

Introduction

The role of ancillary functionalities toward the chemical, electrochemical, and photophysical aspects of the $\text{Ru}(\text{trpy})$ core (trpy = 2,2':6',2''-terpyridine) has been scrutinized in detail in recent years, and it shows substantial variations in properties depending on the electronic nature of the ancillary ligands.¹ As a part of our ongoing program of investigating the role of azo–imine-based ancillary ligands toward the

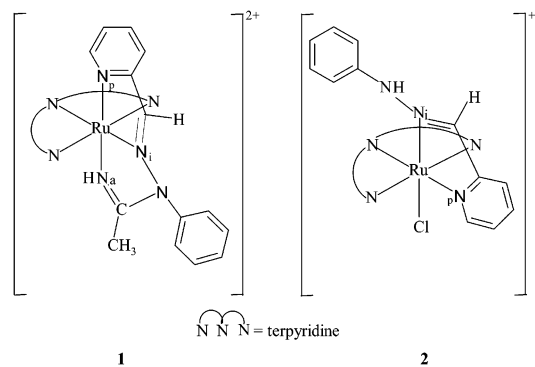
physicochemical properties of the ruthenium monoterpyridine complexes,^{1a–d} the present work deals with the pyridine-derived imine moiety $\text{N}_p\text{C}_5\text{H}_4\text{—CH=N—N}_i\text{—NH—C}_6\text{H}_5$, L, (N_p = pyridine nitrogen, and N_i = imine nitrogen) incorporating an NH spacer between the imine nitrogen and the pendant phenyl ring. The reaction of ruthenium–terpyridine precursor $[\text{Ru}(\text{trpy})\text{Cl}_3]$, with L, leads to the simultaneous formation of an unexpected product, $[\text{Ru}^{\text{II}}(\text{trpy})(\text{L}')^{2+}]$ (**1**), where $\text{L}' = \text{N}_p\text{C}_5\text{H}_4\text{—CH=N—N}_i\text{—N}(\text{C}_6\text{H}_5)\text{—C}(\text{CH}_3)=\text{N}_a\text{H}$ (N_a = amidine nitrogen), representing a new class of coordinated tridentate (N_p , N_i , N_a) ligand comprising an unusual combination of imine and amidine fragments in the

* To whom correspondence should be addressed. E-mail: lahiri@ether.chem.iitb.ernet.in.

[†] Indian Institute of Technology.

[‡] National Chemical Laboratory.

same ligand framework (L') and the expected normal product $[Ru^II(trpy)(L)(Cl)]^+$ (**2**). Although ruthenium–amidine complexes have been reported to be synthesized either via the reaction of amine with the coordinated stable acetonitrile derivative or the reaction of the preformed stable amidine ligands with the suitable ruthenium starting materials,² the present system illustrates a unique example of a highly geometry controlled ruthenium–amidine formation process which presumably proceeds via the in situ generated unstable nitrile intermediate.



Herein, we report the synthesis, spectroelectrochemical properties, and crystal structures of all three members, the free ligand (**L**) and the complexes (**1** and **2**). The role of geometrical configuration of the initially coordinated potentially bidentate unsymmetric ligand **L** toward the transformation process, $L \rightarrow L'$, in **1** has been noted.

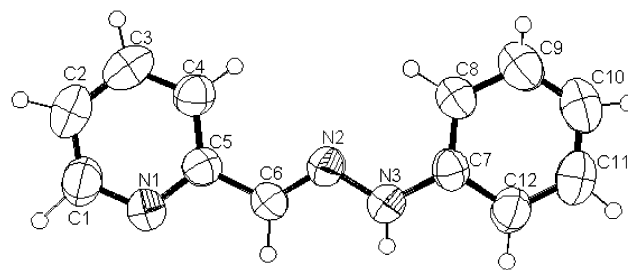


Figure 1. ORTEP diagram of $N_pC_5H_4CH=N_i-NH-C_6H_5$ (**L**). Ellipsoids are drawn at 50% probability.

Results and Discussion

The ligand $N_pC_5H_4-CH=N_i-NH-C_6H_5$ (**L**) (N_p = pyridine nitrogen, and N_i = imine nitrogen) was prepared by condensation of 2-pyridinecarboxaldehyde with phenyl hydrazine in a 1:1 molar ratio in absolute ethanol. In addition to satisfactory elemental analysis (Experimental Section), the single-crystal X-ray structure of **L** has been obtained (Figure 1). It shows intermolecular hydrogen bonding between the NH proton of one **L** and the pyridine nitrogen (N_p) of the nearby other **L** [Supporting Information (Figure S1)] [$D-H$, 0.8394 Å; $H\cdots A$, 2.1784 Å; $D-H\cdots A$, 166.04°]. The bond distances and angles are listed in Table 1, which agree well with the standard reported values. The 1H NMR spectrum of **L** in $CDCl_3$ is consistent with the calculated number of signals, though all the signals are not resolved individually [Supporting Information (Figure S2)].

The reaction of **L** ($N_pC_5H_4-CH=N_i-NH-C_6H_5$) with the ruthenium–terpyridine precursor $Ru(trpy)Cl_3$, in ethanol, afforded a dark solution initially, from which a dark solid mass was isolated on addition of excess saturated aqueous $NaClO_4$ solution. Chromatographic purification of the crude product on a neutral alumina column using a CH_3CN/CH_2Cl_2 mixture (1:4) as eluent resulted in initially an orange complex (**1**) (yield, 40%) followed by a pink complex (**2**) (yield, 50%) as their perchlorate salts.

The formations of **1** and **2** have been authenticated by their single-crystal X-ray structures (see later). In bis-chelated **1**, the preformed potentially bidentate ancillary ligand $N_pC_5H_4-CH=N_i-NH-C_6H_5$ (**L**) has been selectively transformed into a new class of pyridine-based tridentate ligand comprising an unusual combination of imine–amidine functions [$N_pC_5H_4-CH=N_i-N(C_6H_5)-C(CH_3)=N_aH$, (L')]. On the other hand, in **2**, the ancillary ligand (**L**) binds to the ruthenium ion in the expected bidentate manner (N_p , N_i) where the sixth coordination site (Cl^-) is cis to the pyridine nitrogen (N_p) of **L**, which in effect places the active NH function of **L** far away from the chloride group. It is important to note that, unlike complex **2**, the corresponding sixth coordination site, i.e., amidine nitrogen (N_a) in **1**, is trans to the pyridine nitrogen (N_p) of L' . It is significant that, under identical experimental conditions but in the absence of metal fragment $[Ru(trpy)Cl_3]$, the free ligand (**L**) fails to undergo the transformation to L' even in the presence of boiling CH_3CN . This implies that the coordination of **L** to the $Ru(trpy)Cl$ core takes place prior to the transformation process. Moreover, the observed high stability of isolated

- (1) (a) Mondal, B.; Walawalkar, M. G.; Lahiri, G. K. *J. Chem. Soc., Dalton Trans.* **2000**, 4209. (b) Mondal, B.; Paul, H.; Puranik, V. G.; Lahiri, G. K. *J. Chem. Soc., Dalton Trans.* **2001**, 481. (c) Mondal, B.; Chakraborty, S.; Munshi, P.; Walawalkar, M. G.; Lahiri, G. K. *J. Chem. Soc., Dalton Trans.* **2000**, 2327. (d) Chanda, N.; Mondal, B.; Puranik, V. G.; Lahiri, G. K. *Polyhedron*, in press. (e) Pramanik, N. C.; Pramanik, K.; Ghosh, P.; Bhattacharya, S. *Polyhedron* **1998**, *17*, 1525. (f) Gerli, A.; Reedijk, J.; Lakin, M. T.; Spek, A. L. *Inorg. Chem.* **1995**, *34*, 1836. (g) Catalano, V. J.; Heck, R. A.; Immoos, C. E.; Ohman, A.; Hill, M. G. *Inorg. Chem.* **1998**, *37*, 2150. (h) Catalano, V. J.; Heck, R. A.; Ohman, A.; Hill, M. G. *Polyhedron*, **2000**, *19*, 1049. (i) Takeuchi, K. J.; Thompson, M. S.; Pipes, D. W.; Meyer, T. *J. Inorg. Chem.* **1984**, *23*, 1845. (j) Rasmussen, S. C.; Ronco, S. E.; Mlsna, D. A.; Billadeau, M. A.; Pennington, W. T.; Kolis, J. W.; Petersen, J. D. *Inorg. Chem.* **1995**, *34*, 821. (k) Dovelotoglou, A.; Adeyemi, S. A.; Meyer, T. *J. Inorg. Chem.* **1996**, *35*, 4120. (l) Indelli, M. T.; Bignozzi, C. A.; Scandola, F.; Collin, J. P. *Inorg. Chem.* **1998**, *37*, 6084. (m) Lebeau, E. L.; Adeyemi, S. A.; Meyer, T. *J. Inorg. Chem.* **1998**, *37*, 6476. (n) Nazeeruddin, Md. K.; Zakeeruddin, S. M.; Baker, R. H.; Kaden, T. A.; Gratzel, M. *Inorg. Chem.* **2000**, *39*, 4542. (o) Suen, H. F.; Wilson, S. W.; Pomerantz, M.; Walsh, J. L. *Inorg. Chem.* **1989**, *28*, 786. (p) Kelson, E. P.; Phengsy, P. P. *J. Chem. Soc., Dalton Trans.* **2000**, 4023. (q) Hirano, T.; Ueda, K.; Mukaida, M.; Nagao, H.; Oi, T. *J. Chem. Soc., Dalton Trans.* **2001**, 2341.
- (2) (a) Clark, T.; Robinson, S. D. *J. Chem. Soc., Dalton Trans.* **1993**, 2827. (b) Syamala, A.; Chakravarty, A. R. *Inorg. Chem.* **1991**, *30*, 4699. (c) Storhoff, B. N.; Lewis, H. C., Jr. *Coord. Chem. Rev.* **1977**, *23*, 1. (d) Lopez, J.; Santos, A.; Romero, A.; Echavarren, A. M. *J. Organomet. Chem.* **1993**, *443*, 221. (e) Romero, A.; Vegas, A.; Santos, A. *J. Organomet. Chem.* **1986**, *310*, C8. (f) Clark, T.; Robinson, S. D. *Polyhedron* **1992**, *11*, 993. (g) Yamaguchi, Y.; Nagashima, H. *Organometallics* **2000**, *19*, 725. (h) Clark, T.; Robinson, S. D.; Mazid, M. A.; Hursthouse, M. B. *Polyhedron* **1994**, *13*, 175. (i) Breckenridge, S. M.; Carty, A. J.; Pellinghelli, M. A.; Tiripicchio, A.; Sappa, E. *J. Organomet. Chem.* **1994**, *471*, 211. (j) Kondo, H.; Yamaguchi, Y.; Nagashima, H. *J. Am. Chem. Soc.* **2001**, *123*, 500. (k) Clark, T.; Robinson, S. D.; Tocher, D. A. *J. Chem. Soc., Dalton Trans.* **1992**, 3199. (l) Cotton, F. A.; Wilkinson, G.; Murillo, C. A.; Bochmann, M. *Advanced Inorganic Chemistry*, 6th ed.; John Wiley and Sons: New York, 1999; pp 359–360.

Table 1. Selected Bond Distances (Å) and Angles (deg) for NC₅H₄CH=N–NH–C₆H₅ (L), [Ru^{II}(trpy)(L')](ClO₄)₂ (**1**), and [Ru^{II}(trpy)(L)](ClO₄)·CH₃OH (**2**)^a

L		1		2	
N(1)–C(5)	1.336(3)	Ru(1)–N(1)	2.073(3)	Ru(1)–N(1)	2.058(6)
N(1)–C(1)	1.338(3)	Ru(1)–N(2)	1.978(4)	Ru(1)–N(2)	1.958(6)
C(5)–C(6)	1.448(3)	Ru(1)–N(3)	2.080(3)	Ru(1)–N(3)	2.081(6)
C(6)–N(2)	1.275(3)	Ru(1)–N(4)	2.079(3)	Ru(1)–N(4)	2.092(6)
N(2)–N(3)	1.356(3)	Ru(1)–N(5)	1.960(4)	Ru(1)–N(5)	2.039(6)
N(3)–C(7)	1.387(3)	Ru(1)–N(6)	2.087(3)	Ru(1)–Cl	2.403(2)
C(7)–C(8)	1.384(3)	C(20)–C(21)	1.453(5)	C(20)–C(21)	1.430(11)
		C(21)–N(5)	1.302(5)	C(21)–N(5)	1.293(9)
		N(5)–N(7)	1.409(4)	N(5)–N(6)	1.390(9)
		N(7)–C(22)	1.393(5)	N(6)–C(22)	1.425(10)
		C(22)–C(23)	1.513(6)		
		C(22)–N(6)	1.261(6)		
C(5)–N(1)–C(1)	118.5(2)	N(5)–Ru(1)–N(2)	176.20(12)	N(2)–Ru(1)–N(5)	101.5(22)
N(1)–C(1)–C(2)	123.2(3)	N(5)–Ru(1)–N(1)	102.95(14)	N(2)–Ru(1)–N(1)	79.6(2)
N(1)–C(5)–C(6)	115.2(2)	N(2)–Ru(1)–N(1)	79.31(14)	N(5)–Ru(1)–N(1)	94.2(2)
C(6)–N(2)–N(3)	117.0(2)	N(5)–Ru(1)–N(4)	78.46(13)	N(2)–Ru(1)–N(3)	79.1(2)
C(5)–C(6)–N(2)	121.5(2)	N(2)–Ru(1)–N(4)	98.58(13)	N(5)–Ru(1)–N(3)	89.4(2)
N(2)–N(3)–C(7)	120.5(2)	N(1)–Ru(1)–N(4)	89.71(13)	N(1)–Ru(1)–N(3)	158.7(3)
C(7)–C(8)–C(9)	119.9(3)	N(5)–Ru(1)–N(3)	99.19(14)	N(2)–Ru(1)–N(4)	178.4(3)
		N(2)–Ru(1)–N(3)	78.57(14)	N(5)–Ru(1)–N(4)	77.2(2)
		N(1)–Ru(1)–N(3)	157.85(15)	N(1)–Ru(1)–N(4)	101.3(3)
		N(4)–Ru(1)–N(3)	94.58(12)	N(3)–Ru(1)–N(4)	99.9(2)
		N(5)–Ru(1)–N(6)	77.73(14)	N(2)–Ru(1)–Cl(1)	87.38(17)
		N(2)–Ru(1)–N(6)	105.39(13)	N(5)–Ru(1)–Cl(1)	170.94(18)
		N(1)–Ru(1)–N(6)	91.29(13)	N(1)–Ru(1)–Cl(1)	88.95(17)
		N(4)–Ru(1)–N(6)	155.77(16)	N(3)–Ru(1)–Cl(1)	90.69(16)
		N(3)–Ru(1)–N(6)	93.55(13)	N(4)–Ru(1)–Cl(1)	93.85(19)
		C(20)–C(21)–N(5)	112.9(4)	C(20)–C(21)–N(5)	118.5(7)
		C(21)–N(5)–N(7)	123.1(4)	C(21)–N(5)–N(6)	116.9(6)
		N(5)–N(7)–C(22)	111.9(3)	N(5)–N(6)–C(22)	115.9(6)
		N(7)–C(22)–N(6)	119.1(4)		

^a ESD values in parentheses.

normal product **2** particularly in the presence of the nitrile source (CH₃CN) indicates that the initial geometry of L in the complex moieties (**1** and **2**) (maintaining the usual meridional mode of the symmetric terpyridine group) provides the necessary pathways in facilitating the transformation process (see later).

Complexes **1** and **2** exhibit satisfactory elemental analyses and show 1:2 and 1:1 conductivities, respectively, in acetonitrile solution (see Experimental Section). The NH stretching frequencies of the coordinated L' in **1** and coordinated L in **2** are observed at 3236 and 3300 cm⁻¹, respectively.^{2e,3} The perchlorate vibrations are appeared near 1100 and 625 cm⁻¹.

The crystal structures of **1** and **2** are shown in Figures 2 and 3. Selected bond distances and angles are listed in Table 1. The usual meridional mode of bonding of the coordinated terpyridine ligand is maintained in both the complexes. The geometrical constraints imposed on the meridional configuration of the terpyridine ligand in both **1** and **2** as well as L' in **1** are reflected in the respective trans angles, and consequently, the Ru(1)–N(2) (central pyridine nitrogen of terpyridine) distances in **1** and **2** and the Ru(1)–N(5) [central imine nitrogen (N_i) of L'] distance in **1** are approximately 0.1 Å shorter than the terminal Ru–N bonds of the respective tridentate ligands (Table 1).⁴ The Ru^{II}(1)–N(5) (imine) distance in **1**, 1.960(4) Å, is much shorter than the Ru^{II}–

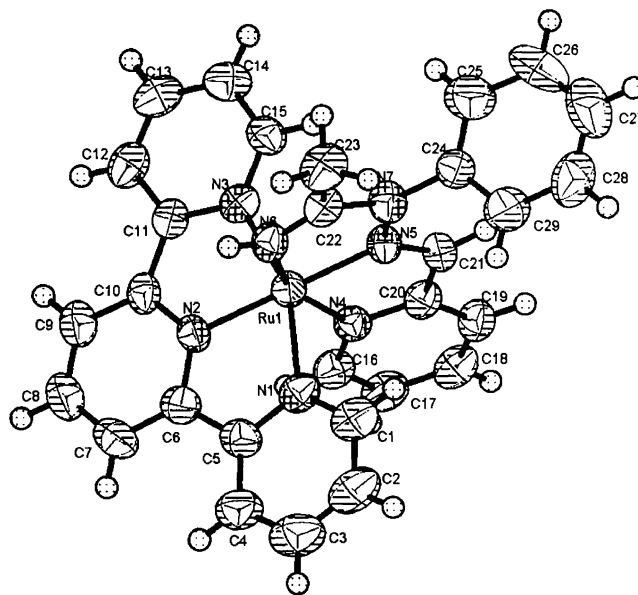


Figure 2. ORTEP diagram of [Ru^{II}(trpy)(L')](ClO₄)₂ (**1**). Perchlorate anions are removed for clarity. Ellipsoids are drawn at 50% probability.

N(imine) distance observed in **2** [2.039(6) Å] and in other reported related complexes (2.04–2.05 Å),^{1d,5} which is possibly because of the involved geometrical constraints in the meridional configuration of the tridentate L' in **1**. The sixth coordinating ligands, that is, amidine nitrogen (N_a) in **1** and Cl⁻ in **2**, are in trans and cis configurations with respect

(3) Jones, C. J.; McCleverty, J. A.; Rothin, A. S. *J. Chem. Soc., Dalton Trans.* **1986**, 109.

(4) (a) Spek, A.; Gerli, A.; Reedijk, J. *Acta Crystallogr., Sect. C* **1994**, *50*, 394. (b) Grover, N.; Gupta, N.; Singh, P.; Thorp, H. H. *Inorg. Chem.* **1992**, *31*, 2014.

(5) (a) Chakraborty, S.; Walawalkar, M. G.; Lahiri, G. K. *Polyhedron* **2001**, *20*, 1859. (b) Boelrijk, A. E. M.; Reedijk, J. *J. Mol. Catal.* **1994**, *89*, 63.

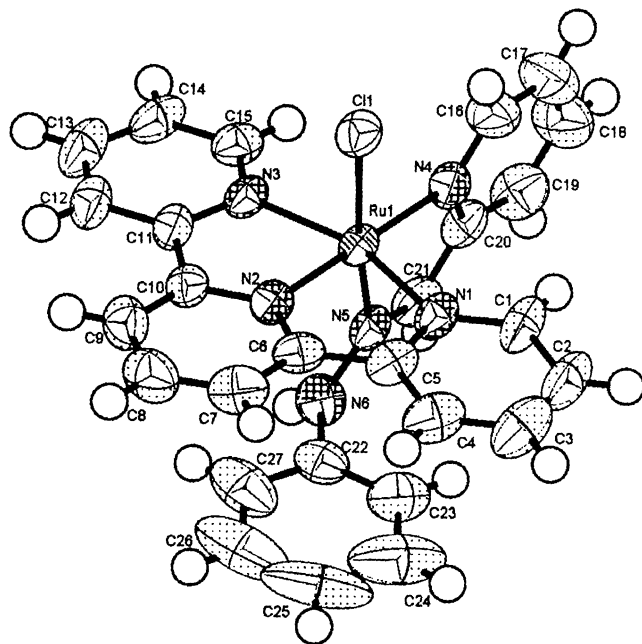


Figure 3. ORTEP diagram of $[\text{Ru}^{\text{II}}(\text{trpy})(\text{L})\text{Cl}](\text{ClO}_4) \text{CH}_3\text{OH}$ (**2**). Perchlorate anion and the methanol solvent molecule are removed for clarity. Ellipsoids are drawn at 50% probability.

to the pyridine nitrogen (N_p) of L' and L , respectively. The $\text{Ru}^{\text{II}}(\text{1})-\text{N}(6)$ (amidine nitrogen) distance, 2.087(3) Å in **1**, is comparable to those observed in $[\text{Ru}(\text{CO})(\text{CH}=\text{CHCMe}_3)\{\text{NH}=\text{C}(\text{Me})(\text{Me}_2\text{pz})\}(\text{PPh}_3)_2]^+$ [2.113(6) Å]^{2d} and $[\text{Ru}_2\text{O}(\text{O}_2\text{CC}_6\text{H}_4\text{-}p\text{-OMe})_2\{\text{NH}_2\text{CH}_2\text{CH}_2\text{NHC}(\text{Me})\text{NH}\}_2(\text{PPh}_3)_2]^{2+}$ [2.066(10) Å].^{2b} The observed single bond distance of $\text{N}(7)-\text{C}(22)$, 1.393(5) Å, and double bond distance of $\text{C}(22)-\text{N}(6)$, 1.261(6) Å, are supportive of the structural form of L' in **1**.^{2b, d}

The ^1H NMR spectra of **1** and **2** in $(\text{CD}_3)_2\text{SO}$ [Supporting Information (Figure S2)] show a calculated number of 20 aromatic protons in each case, overlapping between 5.8 and 10 ppm, 11 from the terpyridine group and 9 from the ancillary ligand L' or L . The coordinated amidine NH proton of L' in **1** and the noncoordinated pendant NH proton of L in **2** are observed at 8.8 and 9.38 ppm, respectively, which have as expected disappeared on D_2O exchange. The lower δ value for the amidine proton can be ascribed to the anisotropic effect of the $\text{C}=\text{N}$ group. The methyl signal of L' in **1** appears at 2.0 ppm.

Complexes **1** and **2** exhibit three major transitions in acetonitrile (Experimental Section) (Figure 4). The observed $\text{Ru}(\text{II}) \rightarrow \pi^*$ (trpy) MLCT transition energy⁶ has been substantially blue-shifted (28 nm) while moving from **2** \rightarrow **1** because of the increased ligand field strength of L' in **1** as compared to L in **2**. It may be interesting to note that the MLCT band energy of **1** is almost identical to that of the $[\text{Ru}(\text{trpy})_2]^{2+}$ complex (478 nm in acetonitrile⁷).

The complexes exhibit one quasireversible ruthenium(II)–ruthenium(III) oxidative process each; E°_{298} , V, (ΔE_p , mV)

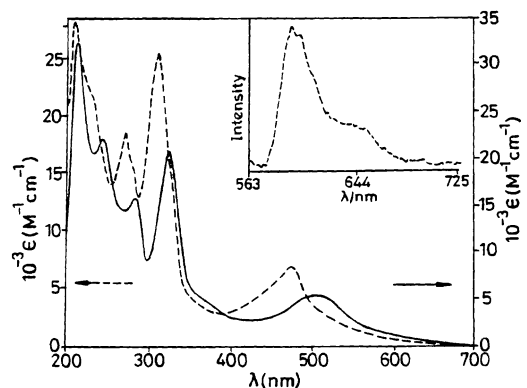


Figure 4. Electronic spectra of $[\text{Ru}^{\text{II}}(\text{trpy})(\text{L}')](\text{ClO}_4)_2$ (**1**) (---) and $[\text{Ru}^{\text{II}}(\text{trpy})(\text{L})\text{Cl}]\text{ClO}_4$ (**2**) (—) in acetonitrile. The inset shows the emission spectrum of **1** in EtOH/MeOH 4:1 (v/v) at 77 K

values are 0.83 (70) for **1** and 0.68 (90) for **2** in acetonitrile versus SCE [Supporting Information (Figure S3)]. Although the oxidation processes are reasonably reversible on the cyclic voltammetric time scale, coulometrically oxidized species, 1^+ and 2^+ , are found to be unstable at 298 K. The potential data are suggestive of higher stability of the ruthenium(II) state in bis-chelated imine–amidine-based complex **1** as compared to imine-based complex **2**. One terpyridine-based reduction has been observed in each case at E°_{298} , V (ΔE_p , mV), values of -1.09 (80) for **1** and -1.12 (100) for **2** versus SCE.⁸

The complexes **1** and **2** are weakly luminescent in methanol/ethanol (1:4) glass at 77 K (Figure 4), exhibiting emission maxima at 598 nm [quantum yield (Φ) = 0.43×10^{-2}] and 574 nm [quantum yield (Φ) = 0.28×10^{-2}], respectively, with vibrational fine structure characteristic of emission from a $^3\text{MLCT}$ excited state presumably involving the terpyridine ligand.^{1a,c,d, 9}

The unsymmetrical nature of L (N_p , N_i) leads to the possibility of the initial formation of two isomeric products of $[\text{Ru}^{\text{II}}(\text{trpy})(\text{L})(\text{Cl})]^+$: trans (**A**) and cis (**B**) with respect to the relative orientations of the pyridine nitrogen (N_p) of L and Cl^- . In the final product **1**, the pyridine nitrogen (N_p) of L' is in trans configuration with respect to the sixth coordination site (amidine nitrogen, N_a), and in **2**, N_p is in cis position with respect to the sixth coordination site (Cl^-). The presence of two possible isomeric structural forms in the final products **1** and **2** implies the initial formation of both the expected trans and cis isomers of $[\text{Ru}^{\text{II}}(\text{trpy})(\text{L})(\text{Cl})]^+$. However, because of built-in structural advantages in the trans isomer (**A**), it underwent subsequent necessary transformations, leading to the formation of amidine derivative **1**.

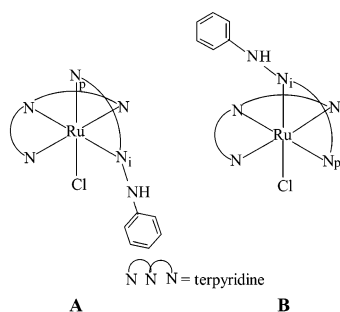
The formation of amidine involves the initial nucleophilic attack of the amine nitrogen onto the carbon center of coordinated nitriles.^{2,10} Because the location of the pendant amine group ($-\text{NH}-\text{C}_6\text{H}_5$) of L in the case of the trans isomer (**A**) is selectively closer to the sixth coordination site,

(6) Bardwell, D. A.; Cargill Thompson, A. M. W.; Jeffery, J. C.; McCleverty, J. A.; Ward, M. D. *J. Chem. Soc., Dalton Trans.* **1996**, 873.

(7) Hecker, C. R.; Gushurst, A. K. I.; McMillin, R. D. *Inorg. Chem.* **1991**, *30*, 538.

(8) (a) Sugimoto, H.; Tsuge, K.; Tanaka, K. *J. Chem. Soc., Dalton Trans.* **2001**, 57. (b) Storrier, G. D.; Colbran, S. B.; Craig, D. C. *J. Chem. Soc., Dalton Trans.* **1998**, 1351.

(9) Chakraborty, S.; Laye, R. H.; Munshi, P.; Paul, R. L.; Ward, M. D.; Lahiri, G. K. *J. Chem. Soc., Dalton Trans.* **2002**, 2348.

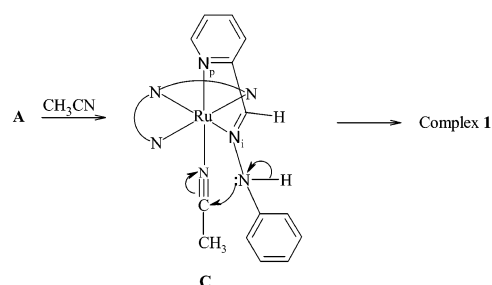


it may therefore be logical to believe that the nucleophilic attack of the suitably placed -NH- function onto the coordinated nitrile center of the in situ generated intermediate $[\text{Ru}^{\text{II}}(\text{trpy})(\text{L})(\text{CH}_3\text{CN})]^{2+}$ (**C**) (Scheme 1) followed by subsequent proton-transfer processes have led to final product **1**. The trans effect of pyridine nitrogen (N_p) of L^{11} in the structural form **A** certainly plays an important role in making the Ru-Cl bond sufficiently labile, which in turn instigates the in situ formation of the proposed nitrile intermediate (**C**) in contact with acetonitrile during the chromatographic workup. On the other hand, the cis orientation of the Ru-Cl bond with respect to N_p of **L** (structure **B**) in **2** makes it inert toward nitrile attack even under boiling conditions. Moreover, the structural form, **B** in **2**, fixes the active NH function of **L** away from the site of concern (i.e., the sixth coordination site), and these in combination essentially stabilize complex **2** in the expected composition.

It should be noted that a similar type of stereoregulated reaction in the ruthenium monoterpyridine core has been reported separately by Constable et al.¹² and Ward et al.,⁶ where, depending on the cis and trans configurations of the $(\text{trpy})\text{Ru-Cl}$ bond relative to the active pendant phenyl ring of the coordinated 6-phenyl-bipyridine, it binds to ruthenium-(II) as an unusual cyclometallating terdentate function giving $[\text{Ru}(\text{trpy})(\text{N},\text{N}',\text{C})]^+$ and as a normal bidentate N,N' -donor giving $[\text{Ru}(\text{trpy})(\text{N},\text{N}')(\text{Cl})]^+$, respectively.

To isolate the most probable intermediate, *trans*- $[\text{Ru}^{\text{II}}(\text{trpy})(\text{L})(\text{Cl})]^+$ (structure **A**), along with the stable *cis*- $[\text{Ru}^{\text{II}}(\text{trpy})(\text{L})(\text{Cl})]^+$ (structure **B**) isomer from the initially obtained reaction mixture, ethyl acetate ($\text{CH}_3\text{COOC}_2\text{H}_5$),

Scheme 1



acetone (CH_3COCH_3), as well as methanol (CH_3OH) solvents were tested instead of using nitrile-based eluent (CH_3CN) during the chromatographic purification process but failed to separate the products.

Conclusion

We have thus observed that the reaction of $\text{Ru}(\text{trpy})\text{Cl}_3$ with the pyridine-based imine function $\text{N}_p\text{C}_5\text{H}_4\text{-CH=N}_i\text{-NH-C}_6\text{H}_5$ (**L**), incorporating an NH spacer between the imine group (N_i) and the pendant phenyl ring, leads to the simultaneous formation of two products $[\text{Ru}(\text{trpy})(\text{L}')^{2+}$ (**1**) and $[\text{Ru}(\text{trpy})(\text{L})\text{Cl}]^+$ (**2**). In **1**, the imine-based potentially bidentate ligand (**L**) has been selectively transformed into a new class of tridentate ligand comprising an unusual combination of imine-amidine functions, $[\text{N}_p\text{C}_5\text{H}_4\text{-CH=N}_i\text{-N}(\text{C}_6\text{H}_5)\text{C}(\text{CH}_3)=\text{N}_a\text{H}$, L'], although the identity of the free ligand (**L**) remains unaltered in complex **2**. The trans configuration of the Ru-N_a (amidine nitrogen) bond with respect to the pyridine nitrogen (N_p) of L' in **1** in contrast to the cis configuration of the corresponding Ru-Cl bond in **2** provides clear evidence that the formation of amidine in **1** is a highly stereoregulated operation.

Experimental Section

The starting complex, $\text{Ru}(\text{trpy})\text{Cl}_3$, was prepared according to the reported procedure.^{1b} 2,2':6',2''-Terpyridine, phenyl hydrazine, and 2-pyridinecarboxaldehyde were obtained from Aldrich. Other chemicals and solvents were reagent grade and used as received. For spectroscopic and electrochemical studies, HPLC grade solvents were used. Commercial tetraethylammonium bromide was converted into pure tetraethylammonium perchlorate by following an available procedure.¹³

UV-vis spectra were recorded with a Shimadzu-2100 spectrophotometer. FT-IR spectra were taken on a Nicolet spectrophotometer with samples prepared as KBr pellets. Solution electrical conductivity was checked using a Systronic 305 conductivity bridge. Magnetic susceptibility was checked with a PAR vibrating sample magnetometer. ^1H NMR spectra were obtained with a 300 MHz Varian FT spectrometer. Cyclic voltammetric, differential pulse voltammetric, and coulometric measurements were carried out using a PAR model 273A electrochemistry system. Platinum wire working and auxiliary electrodes and an aqueous saturated calomel reference electrode (SCE) were used in a three electrode configuration. The supporting electrolyte was $[\text{NEt}_4]\text{ClO}_4$, and the solute concentration was $\sim 10^{-3}$ M. The half-wave potential $E_{0.298}^\circ$ was set equal to $0.5 \cdot (E_{pa} + E_{pc})$, where E_{pa} and E_{pc} are anodic and cathodic cyclic

- (10) (a) Du, S.; Kautz, J. A.; McGrath, T. D.; Stone, F. G. A. *J. Chem. Soc., Dalton Trans.* **2002**, 1553. (b) Paul, P.; Nag, K. *Inorg. Chem.* **1987**, *26*, 1586. (c) Tschugaev, L.; Lebedinski, W. *C. R. Hebd. Seances Acad. Sci.* **1915**, *161*, 563. (d) Stephenson, N. C. *J. Inorg. Nucl. Chem.* **1962**, *24*, 801. (e) Buckingham, D. A.; Foxman, B. M.; Sargeson, A. M.; Zanella, A. *J. Am. Chem. Soc.* **1972**, *94*, 1007. (f) Nolan, K. B.; Hay, R. W. *J. Chem. Soc., Dalton Trans.* **1974**, 914. (g) Ros, R.; Renaud, J.; Roulet, R. *J. Organomet. Chem.* **1976**, *104*, 393. (h) Calligaro, L.; Michelin, R. A.; Uguagliati, P. *Inorg. Chim. Acta* **1983**, *76*, L83. (i) Calligaro, L. *Polyhedron* **1984**, *3*, 117. (j) Pinnel, D.; Wright, G. B.; Jordan, R. B. *J. Am. Chem. Soc.* **1972**, *94*, 6104. (k) Maresca, L.; Natile, G.; Intini, F. P.; Gasparini, F.; Tiripicchio, A.; Tiripicchio-Camellini, M. *J. Am. Chem. Soc.* **1986**, *108*, 1180. (l) Edelman, F. T. *Coord. Chem. Rev.* **1994**, *137*, 403.
- (11) (a) Ahmed, E.; Chatterjee, C.; Cooksey, C. J.; Tobe, M. L.; Williams, G.; Humanes, M. *J. Chem. Soc., Dalton Trans.* **1989**, 645. (b) Tobe, M. L. *Adv. Inorg. Bioinorg. Mech.* **1983**, *2*, 76. (c) Tobe, M. L. *Acc. Chem. Res.* **1970**, *3*, 377. (d) Basolo, F.; Bergmann, J. G.; Meeker, R. E.; Pearson, R. G. *J. Am. Chem. Soc.* **1956**, *78*, 2676.
- (12) (a) Constable, E. C.; Cargill Thompson, A. M. W. *New J. Chem.* **1996**, *20*, 65. (b) Constable, E. C.; Cargill Thompson, A. M. W.; Cherryman, J.; Liddiment, T. *Inorg. Chim. Acta* **1995**, *235*, 165. (c) Constable, E. C.; Hannon, M. J. *Inorg. Chim. Acta* **1993**, *211*, 101.

- (13) Sawyer, D. T.; Sobkowiak, A.; Roberts, J. L., Jr. *Electrochemistry for Chemists*; Wiley: New York, 1995.

voltammetric peak potentials, respectively. A platinum wire gauze working electrode was used in coulometric experiments. All experiments were carried out under a dinitrogen atmosphere and were uncorrected for junction potentials. The elemental analyses were carried out with a Carlo Erba (Italy) elemental analyzer. Solution emission properties were checked using a SPEX-fluorolog spectrofluorometer with fluorescence quantum yields being determined using a previously described method.¹⁴

Preparation of $N_pC_5H_4-CH=N_i-NH-C_6H_5$ (L). To a stirred solution of 2-pyridinecarboxaldehyde (1 g, 9.33 mmol) in dry ethanol (15 mL) was added phenyl hydrazine (1.009 g, 9.33 mmol) dropwise. The stirring was continued for 1 h. The solid product thus obtained was collected by filtration and recrystallized from hot ethanol. Yield: 1.654 g (90%). Anal. Calcd (Found) for $C_{12}H_{11}N_3$: C, 73.09 (73.38); H, 5.58 (5.41); N, 21.32 (20.97).

Synthesis of $[Ru(trpy)(L)](ClO_4)_2$ (1) and $[Ru(trpy)(L)(Cl)]ClO_4$ (2). Initially, the starting complex, $Ru(trpy)Cl_3$ (100 mg, 0.23 mmol), in 25 mL of ethanol was heated at reflux for 10 min. The ligand L, (45.31 mg, 0.23 mmol) followed by LiCl (39 mg, 0.92 mmol) and NEt_3 (0.16 mL, 1.15 mmol), was added to the hot solution containing the metal precursor, and the resulting mixture was heated to reflux for 8 h. The solvent was then removed under reduced pressure. The dry mass thus obtained was dissolved in a minimum volume of methanol, and an excess saturated aqueous solution of $NaClO_4$ was added to it. The crystalline product thus obtained was filtered off and washed thoroughly with cold methanol followed by ice-cold water. The product was dried in vacuo over P_4O_{10} . It was then passed through the alumina (neutral) column. With CH_2Cl_2/CH_3CN (4:1), an orange solution corresponding to **1** was separated initially. Complex **2** was eluted next by CH_2Cl_2/CH_3CN (2:1). Evaporation of solvent under reduced pressure afforded pure complexes **1** and **2**. Yield: **1**, 71 mg (40%); **2**, 76.5 mg (50%). Anal. Calcd (Found) for **1**: C, 45.14 (45.37); H, 3.24 (3.39); N, 12.71 (12.83). Anal. Calcd (Found) for **2**: C, 48.66 (48.28); H, 3.33 (3.51); N, 12.61 (12.59). Molar conductivity [Λ_M ($\Omega^{-1} cm^2 M^{-1}$)] in acetonitrile: 234 for **1** and 123 for **2**. λ_{max}/nm ($\epsilon/M^{-1} cm^{-1}$): for **1**, 476 (6938), 308 (25416), 272 (18477); for **2**, 504 (5253), 317 (20610), 275 (15587).

Crystal Structure Determination. Single crystals of L were grown by slow diffusion of a dichloromethane solution of it in hexane followed by slow evaporation. X-ray data of L were collected on a PC-controlled Enraf-Nonius CAD-4 (MACH-3) single-crystal X-ray diffractometer using Mo $K\alpha$ radiation. Significant crystallographic parameters are listed in Table 2. The structures were solved and refined by full-matrix least-squares on F^2 using SHELX-97 (SHELXTL).¹⁵

Single crystals of **1** were grown by slow diffusion of a dichloromethane solution of it in petroleum ether (bp 60–80 °C) followed by slow evaporation, and for **2**, an acetonitrile solution

Table 2. Crystallographic Data for $NC_5H_4CH=N-NH-C_6H_5$ (L), $[Ru^{II}(trpy)(L)](ClO_4)_2$ (**1**), and $[Ru^{II}(trpy)(L)](ClO_4)\cdot CH_3OH$ (**2**)

	L	1	2
molecular formula	$C_{24}H_{22}N_6$	$C_{29}H_{25}Cl_2N_7O_8Ru$	$C_{28}H_{26}Cl_2N_6O_3Ru$
fw	394.48	771.53	698.52
radiation	Mo $K\alpha$	Mo $K\alpha$	Mo $K\alpha$
temp/ K	293(2)	293(2)	293(2)
cryst symmetry	monoclinic	monoclinic	monoclinic
space group	<i>Cc</i>	<i>P2₁/c</i>	<i>P2₁/c</i>
<i>a</i> /Å	24.258(2)	14.934(8)	8.879(2)
<i>b</i> /Å	7.0860(7)	17.757(9)	25.991(6)
<i>c</i> /Å	14.3020(18)	12.402(7)	13.059(3)
β (deg)	119.065(8)	111.049(8)	94.317(4)
<i>V</i> /Å ³	2148.8(4)	3069(3)	3004.9(12)
<i>Z</i>	4	4	4
μ/mm^{-1}	0.76	0.748	0.747
<i>D</i> _{calcd} /g cm ⁻³	1.219	1.670	1.544
<i>R</i>	0.0534	0.0598	0.0718
<i>R</i> _w	0.1293	0.1327	0.1705

of it was allowed to diffuse slowly in benzene followed by slow evaporation. Crystal data and data collection parameters are given in Table 2. X-ray data of **1** and **2** were collected on a Bruker SMART APEX CCD diffractometer using Mo $K\alpha$ radiation. The structures were solved and refined by full-matrix least-squares on F^2 using SHELX-97 (SHELXTL).¹⁵ SADABS correction was applied. All the data were corrected for Lorentzian, polarization, and absorption effects. Hydrogen atoms were included in the refinement process as per the riding model.

The two perchlorate moieties in **1** are disordered. Several C–H \cdots O and N–H \cdots O hydrogen bonds and C–H π interactions have been observed in the crystal structure of **1**.

The molecular structure of complex **2** contains the perchlorate anion and methanol as solvent of crystallization in the ratio 1:1:1. Oxygen atoms of the perchlorate moiety and CH_3OH solvent are disordered. The benzene moiety (C24, 25, etc.) is also disordered. There is an intramolecular C–H \cdots Cl interaction and several C–H \cdots O, C–H \cdots N and N–H \cdots O hydrogen bonds which essentially stabilize the structure.

Acknowledgment. We thank the Council of Scientific and Industrial Research, New Delhi, for the financial support. The X-ray structural studies for the ligand (L) were carried out at the National Single Crystal Diffractometer Facility, Indian Institute of Technology, Bombay. Special acknowledgment is made to the Regional Sophisticated Instrumentation Center, RSIC, Indian Institute of Technology, Bombay, for providing the NMR facility. The referees' comments at the revision stage were very helpful.

Supporting Information Available: X-ray crystallographic data for the ligand (L) and complexes **1** and **2**· CH_3OH in CIF format. Hydrogen bonding pattern of L (Figure S1). ¹H NMR spectra of L, **1**, and **2** (Figure S2). Cyclic voltammograms of **1** and **2** (Figure S3). This material is available free of charge via the Internet at <http://pubs.acs.org>.

IC020351+

(14) (a) Alsfasser, R.; Eldrik, R. V. *Inorg. Chem.* **1996**, *35*, 628. (b) Chen, P.; Deusing, R.; Graff, D. K.; Meyer, T. J. *J. Phys. Chem.* **1991**, *95*, 5850. (c) Crosby, G. A.; Elfring, W. H., Jr. *J. Phys. Chem.* **1976**, *80*, 2206.

(15) Sheldrick, G. M. *SHELX-97 program for crystal structure solution and refinement*; University of Göttingen: Göttingen, Germany, 1997.